Adsorption 3, 267–275 (1997)

Equilibria and Kinetics Characterisation of Two Different Structured Nutshell—Derived Activated Carbons

K. WANG, A. AHMADPOUR AND D.D. DO
Department of Chemical Engineering, The University of Queensland, Brisbane QLD 4072

Received May 13, 1996; Revised October 9, 1996; Accepted October 16, 1996

Abstract. Adsorption equilibria and dynamics of *n*-butane on two activated carbon samples prepared from the physical activation of nutshell are studied in this paper. The micropore size distribution (MPSD) is considered as the main source of solid heterogeneity. Lennard-Jones' potential theory and Dubinin's theory (TVFM) are used in the equilibria data to derive the MPSD, which is well fitted by a Gamma distribution function. The adsorption energy distribution derived from the MPSD is very asymmetric for both the samples studied, and this energy distribution is used in the HMSD/HMSMD kinetics models for the study of adsorption dynamics of *n*-butane.

Keywords: characterisation, equilibria, kinetics, micropore size distribution, *n*-butane, nutshell

1. Introduction

Activated carbons obtained from different carbonisation and activation processes exhibit different structures (Ahmadpour and Do, 1995). At the microscopic level, the activated carbon is composed of amorphous carbon and graphitic crystalline units. The former provides pores for intercrystalline transport (macropores), while the latter provides channel networks (micropores) in which most adsorption capacity resides. The basic structure of crystalline units is graphitic-like aromatic microcrystallities, which accommodate slit-shaped micropores between graphitic layers (pore walls). As a result, the overall adsorption equilibrium and dynamics on activated carbon could be characterised by the micropore size distribution (MPSD) of slit-shaped pores (Jagiello and Schwartz, 1992, 1993; Everett and Powl, 1976; Hu and Do, 1994), although in reality, the defects and functional groups may also have some influences on both the equilibria and kinetics. Dubinin (1965) considered the physical adsorption inside the slit pores and concluded that the volume of micropores and supermicropores is filled by the adsorbed molecules in accordance with their respective adsorption force fields and the interaction among them. This mechanism is termed as the theory of volume filling of micropores (TVFM) (Dubinin, 1989).

To characterise the structure of an activated carbon has always been a topic of great interest. Although many methods have been proposed to address this problem, but up to now, no well developed theory is available (Stoeckli, 1989; Russell and LeVan, 1994). In this paper, adsorption equilibria and dynamics of *n*-butane on two different structured activated carbons derived from nutshell are employed to study the MPSD, which is considered to be the main source of solid heterogeneity and the distinguishing characteristics of carbon structure. The detailed procedures of preparing these two carbons are described in Nguyen et al. (1995).

2. Theory

Solid heterogeneity in activated carbon is assumed to be attributed to the pore size distribution of slit-shaped micropores, which results in a distribution of adsorption potential. This potential is described by the dispersion force between the adsorbate molecule and molecules on the pore walls. Thus knowing the MPSD of an adsorbent from the equilibria analysis,

the corresponding adsorption energy distribution can be derived and it could be used to analyse the adsorption dynamics (Hu and Do, 1994).

2.1. *Slit-Pore Potential*

In physical adsorption, the main interaction between adsorbate molecule and each carbon molecule in the graphitic layers is the dispersive force, which can be described by the Lennard-Jones' 12-6 potential. The overall potential of a molecule confined in a slit pore is the integral of this 12-6 potential over both pore walls. The final form is the so-called 10-4 potential (Everett and Powl, 1976):

$$U_p(z) = \frac{5}{3}U_s^*\left[\frac{2}{5}\left(\frac{\sigma_{12}}{z}\right)^{10} - \left(\frac{\sigma_{12}}{z}\right)^4 + \frac{2}{5}\left(\frac{\sigma_{12}}{2r-z}\right)^{10} - \left(\frac{\sigma_{12}}{2r-z}\right)^4\right]. \quad (1)$$

where z is the distance between the molecule and one of the pore walls, r is the pore half-width, σ_{12} is the collision diameter and U_s^* is the depth of Lennard-Jones potential minimum between an adsorbate molecule and a single graphite lattice. The adsorption energy, which is taken as the negative of this potential minimum, ranges from U_s^* (corresponding to $r \to \infty$) to $2U_s^*$ (corresponding to $r = \sigma_{12}$), as a function of pore-width. Using Eq. (1), the adsorption energy distribution then can be calculated from a given micropore size distribution.

2.2. *Isotherm and Micropore Size Distribution*

The heterogeneous surface of an activated carbon can be assumed as the combination of many small homogeneous patches, of which in each patch micropores of the same size are grouped together. At adsorption equilibrium, all patches are in local equilibrium with the gas phase, thus, we can write the equation for the overall amount adsorbed as an integral of the local isotherm over the range of micropores as follows:

$$C_\mu = C_{\mu s}\int_{r_{\min}}^{\infty} \theta(r, P, T) f(r)\, dr \quad (2)$$

where $\theta(r, P, T)$ is the local isotherm, $f(r)$ is the micropore size distribution function and $r_{\min}$ is the minimum accessible pore half-width. In this paper, the value of $r_{\min}$ is taken as $0.8885\sigma_{12}$, so that the adsorbates inside the pores having this pore half-width would have the same adsorption potential as those interacting with a flat surface. This is because for pores having half-width less than $0.8885\sigma_{12}$ the interaction energy is less than that of a flat surface, and as a result adsorbate molecules would adsorb preferentially on flat surface rather than in those pores. The micropore size distribution $f(r)$ is assumed to take the form of either the Gaussian distribution:

$$f(r) = \frac{1}{\delta\sqrt{2\pi}}\exp\left[-\frac{(r-r^*)^2}{2\delta^2}\right] \quad (3)$$

or the Gamma distribution:

$$f(r) = \frac{q^{\gamma+1}r^\gamma e^{-qr}}{\Gamma(\gamma+1)} \quad (4)$$

The local adsorption isotherms $\theta(r, P, T)$ is assumed to take the form of either Langmuir equation or the DA equation. The Langmuir equation has the following f orm:

$$C_\mu(r, T, P) = \frac{W_0}{V_{(T)}}\frac{\mathrm{Pb}[E(r)]}{1+\mathrm{Pb}[E(r)]} \quad (5a)$$

where $b[E(r)]$ is the local adsorption affinity of the patch having an interaction energy E, which is a function of the micropore half-width:

$$b[E(r)] = b_0\exp\left[\frac{E(r)}{RT}\right] \quad (5b)$$

with b_0 being the adsorption affinity at zero energy level.

The DA equation is:

$$C_\mu(r, T, P) = \frac{W_0}{V_{(T)}}\exp[-(A/E_0)^n] \quad (6a)$$

where A is the free energy of adsorption and is defined as

$$A = -\Delta G = RT\ln(P_s/P) \quad (6b)$$

The parameter $E_0 = \alpha/r$ is the characteristic adsorption energy, and the exponent 'n' is assumed to take the values of 2 and 3 in this paper. It should be noted that Eqs. (5) and (6) assume different adsorption mechanisms in micropores. In Eq. (5), the adsorption energy $E(r)$ is taken as the negative of the potential minimum calculated from Lennard-Jones' 10-4 potential for slit

shaped pores, while in Eq. (6) the characteristic adsorption energy E_0 is assumed to be inversely proportional to the pore half-width. The maximum adsorption capacities in both isotherms are taken as the micropore volume accessible to adsorbate divided by the liquid molar volume of adsorbate at that temperature.

It is also worthwhile to note that the combination of local DA isotherm and gamma pore distribution in Eq. (2) will not result in analytical solution like the J-C isotherm (Jaroniec et al., 1989). Because in this paper, the gamma distribution is assumed to be in terms of pore half-width directly and the pore accessibility is cut at $r_{\min}$.

If the local isotherm takes the form of Langmuir equation and the MPSD takes the Gamma distribution, the overall isotherm of Eq. (2) becomes:

$$C_\mu = \frac{W_0}{V_{(T)}} \int_{0.8885}^{\infty} \frac{\mathrm{Pb}[E(x)]}{1+\mathrm{Pb}[E(x)]} \frac{Q^{\gamma+1} x^\gamma e^{-Qx}}{\Gamma(\gamma+1)} dx \quad (7)$$

where $x = r/\sigma_{12}$ is the reduced pore half-width, and $Q = q\sigma_{12}$ is the new distribution parameter. By minimising the residual between Eq. (7) and experimental data, the optimal isotherm and MPSD parameters can be extracted.

2.3. *Adsorption Energy Distribution and MPSD*

The overall adsorption isotherm on a heterogeneous surface can be expressed in the form of MPSD or adsorption energy distribution:

$$C_\mu = \int_{r_{\min}}^{\infty} \theta(r, T, P) f(r)\, dr = \int_{E_{\min}}^{E_{\max}} \theta(E, T, P) F(E)\, dE \quad (8)$$

where E is the adsorption energy, which is a function of pore size. If it is calculated from 10-4 potential minimum, the relationship between energy distribution and MPSD derived from Eq. (8) is:

$$F(E) = -\frac{f(r)}{\left[dU_r^{\min}/dr\right]} \quad (9)$$

where $U_r^{\min}$ is the pore potential minimum and $E = -U_r^{\min}$ ranges from U_s^* to $2U_s^*$. In Eq. (9), the denominator becomes zero at $r = \sigma_{12}$, so the energy distribution is infinite at this point. To remedy this problem, we split the range of micropore half width into two sections; section I ($0.8885\sigma_{12}$, σ_{12}) and section II (σ_{12}, $3\sigma_{12}$). Therefore, the corresponding adsorption energy will range from U_s^* to $2U_s^*$ in section I, and $2U_s^*$ to U_s^* in section II. Then, the overall isotherm in terms of energy distribution can be written as:

$$C_\mu = -\int_{U_s^*}^{2U_s^*} \theta(E, T, P) \frac{f(r)}{\left[dU_r^{\min}/dr\right]_{\mathrm{I}}} dE - \int_{2U_s^*}^{U_s^*} \theta(E, T, P) \frac{f(r)}{\left[dU_r^{\min}/dr\right]_{\mathrm{II}}} dE \quad (10)$$

Since $[dU_r^{\min}/dr]_{\mathrm{I}} < 0$, Eq. (10) can be rearranged as:

$$C_\mu = \int_{U_s^*}^{2U_s^*} \theta(E, T, P) \times \left\{ \frac{f(r)}{\left|\left[dU_r^{\min}/dr\right]_{\mathrm{I}}\right|} + \frac{f(r)}{\left[dU_r^{\min}/dr\right]_{\mathrm{II}}} \right\} dE \quad (11)$$

This means that the adsorption energy distribution over the whole accessible pore size range is:

$$F(E) = \frac{f(r)}{\left|\left[dU_r^{\min}/dr\right]_{\mathrm{I}}\right|} + \frac{f(r)}{\left[dU_r^{\min}/dr\right]_{\mathrm{II}}} \quad (12)$$

2.4. *Dynamics*

The HMSMD (Heterogenous Macropore, Surface and Micropore Diffusion) model proposed by Hu and Do (1993) is used here for the analysis of the kinetics data. Details of this model can be found in the mentioned paper, but we presented briefly below the necessary equations for the discussion later.

The flux equations for the diffusion process along the particle and microparticle coordinates are:

$$J_\mu[E(r)]_r = -D_\mu[E(r)] \frac{C_\mu[E(r)]}{C_{\mathrm{im}}} \frac{\partial C_{\mathrm{im}}}{\partial r} \quad (13)$$

$$J_\mu[E(r)]_{r_\mu} = -\beta^2 D_\mu[E(r)] \frac{C_\mu[E(r)]}{C_{\mathrm{im}}} \frac{\partial C_{\mathrm{im}}}{\partial r_\mu} \quad (14)$$

where C_{im} is the gas phase concentration which would be in equilibrium with the adsorbed phase concentration C, the parameter β^2 is to characterise the difference in the magnitude of adsorbed phase diffusion in the microparticle coordinate relative to that in the particle. The diffusion coefficient of the adsorbed species $D_\mu[E(r)]$ is the local surface diffusivity at energy level

Table 1. Activation conditions and physical properties of carbon samples.

Sample	Activation agent	Time (min)	Temp. (°C)	Weight loss (%)	Langmuir area (m^2/g)	BET area (m^2/g)	W_{0,N_2} (cc/g)
C3	CO_2	30	800	10	530	358	0.190
C10	CO_2	705	800	65	1700	1262	0.500

W_{0,N_2}: Micropore volume of carbon samples from N_2 adsorption at 77 K.

$E(r)$, defined as:

$$D_\mu[E(r)] = D_{\mu 0} \exp\left[-\frac{aE(r)}{RT}\right] \tag{15}$$

where $D_{\mu 0}$ is the surface diffusivity at zero loading and zero energy level, and $[aE(r)]$ is the local activation energy for surface diffusion. The parameter $D_{\mu 0}$ is the only parameter that we need to extract from the fitting of the dynamics equation with the kinetics data.

The mass balance equation for the concentration distribution in the particle is:

$$\varepsilon_M \frac{\partial C_p}{\partial t} + (1-\varepsilon_M) \times \frac{\int_0^{R_\mu} \frac{\partial}{\partial t}\left\{\int_{E_{\min}}^{E_{\max}} C_\mu[E(r)]F[E(r)]d[E(r)]\right\} r_\mu^{s_\mu} dr_\mu}{\int_0^{R_\mu} r_\mu^{s_\mu} dr_\mu}$$
$$= -\varepsilon_M \frac{1}{r^s}\frac{\partial}{\partial r}(r^s J_p) - (1-\varepsilon_M)\frac{1}{r^s}\frac{\partial}{\partial r} \times \left[r^s \frac{\int_0^{R_\mu} z\left\{\int_{E_{\min}}^{E_{\max}} J_\mu[E(r)]_r F[E(r)]dE(r)\right\} r_\mu^{s_\mu} dr_\mu}{\int_0^{R_\mu} r_\mu^{s_\mu} dr_\mu}\right] \tag{16}$$

where the pore diffusion flux is expressed by the Fickian diffusion equation

$$J_p = -D_e \frac{\partial C_p}{\partial r} \tag{17}$$

where D_e is the effective pore diffusivity, which is calculated from the Kundsen and molecular diffusivities.

3. Experiment

Activated carbons of different structures are prepared from Macadamia nutshell (NS-ACs) by various physical activation procedures (Nguyen et al., 1995). Two samples (C3 and C10) are chosen from the series of carbons activated with CO_2 gas. These samples, one with low carbon burnoff (denoted hereafter as C3) and the other with high burnoff (denoted as C10) are selected in such a way to differ in terms of their internal pore structures. Sample C3 is a carbon in which most of its pores are in the micropore range, while in the C10 sample the mesopores also have some contribution in its pore structure. The activation conditions and physical properties of these two samples are shown in Table 1.

Adsorption isotherms of *n*-butane on each sample are obtained on a high accuracy volumetric rig, and for each sample, isotherm data at 10, 30 and 60°C are collected.

Adsorption dynamics of *n*-butane on each carbon sample is measured on a differential adsorption bed (DAB), whose detailed procedures is described elsewhere (Hu and Do, 1993). Carbon samples are filled into cylindrical copper tubes of various lengths. For each carbon several slab pellets of length 2.2 and 4.5 mm are made, and the pellets of same length are put into the DAB for dynamic experiments.

4. Results and Discussion

4.1. Equilibrium and MPSD

The non-linear optimisation techniques available in MATLAB are employed to derive the isotherm and MPSD parameters by minimising the residuals between the model predictions (Eq. (2)) and the experimental isotherm data. The micropore volume of carbon samples and MPSD parameters are considered to be adsorbent-specific and are assumed to be temperature independent.

Tables 2 and 3 show the parameters derived from local Langmuir isotherm and DA isotherm for the case

Table 2. Isotherm and MPSD parameters derived from Langmuir isotherm and Gamma distribution.

Sample	W_0 (cc/g)	b_0 (k Pa^{-1})	U_s^* (J/mole)	Q	γ
C3	0.2918	2.697E−4	1.205E+4	102.1	95.84
C10	0.6198	2.770E−4	1.199E+4	113.0	131.0

Table 3. Isotherm and MPSD parameters derived from DA isotherm and Gamma distribution.

Sample	W_0 (cc/g)	E_k (J/mole)	Q	γ
C3	0.3345	1.062E+4	110.5	100.7
C10	0.5880	1.516E+4	114.4	119.5

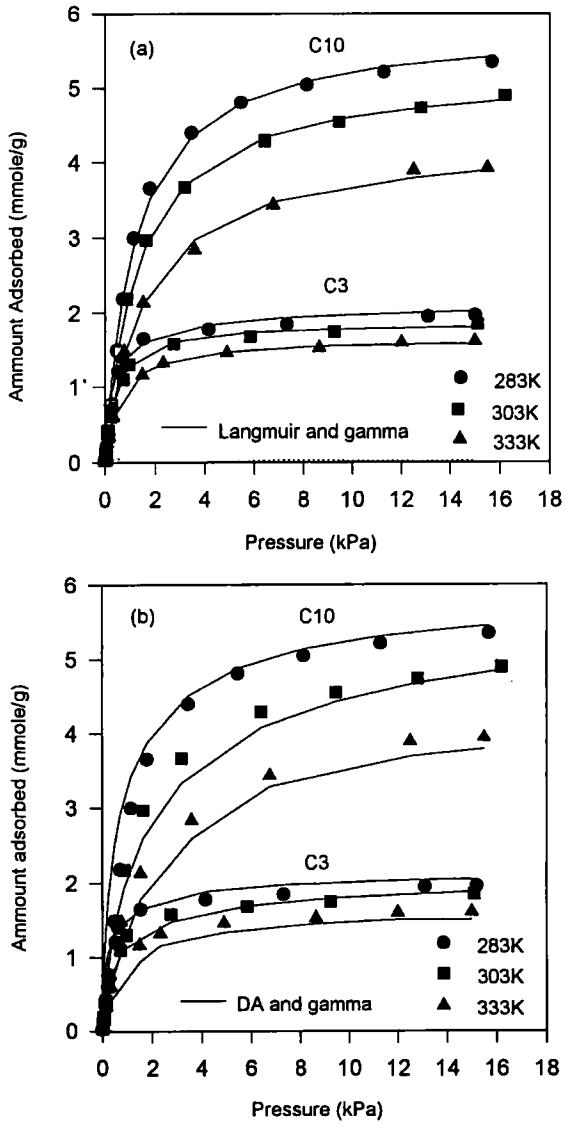

Figure 1. Adsorption isotherm of n-butane (symbols) and model prediction (lines) on two NS-ACs, (a) Langmuir isotherm and Gamma distribution, (b) DA isotherm and Gamma distribution.

of MPSD taking the form of Gamma distribution. The experimental isotherm data and the fitted curves are shown in Fig. 1. The model fitting is generally good when the Langmuir equation is used to as the local adsorption isotherm (Fig. 1(a)), and it is worthwhile to note that b_0 (adsorption affinity at zero energy level) and U_s^* (potential well depth for single lattice) are very comparable for the two activated carbon samples tested. This is physically expected because these parameters should reflect the interaction between the adsorbate molecule and a single lattice layer, and that should be independent of the porous structure.

When the DR equation (that is $n = 2$ in Eq. 6(a)) is used as the local isotherm, the convergence in the optimisation procedure is very poor compared to that for the case of Langmuir local isotherm equation. This suggests that the DR is not a good choice as a local isotherm, at least from the optimisation point of view. However, when the DA equation with $n = 3$ is used instead, better convergence and good fit are observed although the degree of good fit is not as good as that for the case of Langmuir as the local isotherm.

Figure 2(a) shows the micropore distribution of two samples derived from local Langmuir isotherm with Gamma distribution. It can be seen that the MPSD of the activated carbon sample C3 has higher density in the smaller pore size range with the mean reduced half-width of 0.95, while the MPSD of the sample C10 is shifted to the higher pore size range with the mean reduced pore half-width of 1.17. This is in perfect accordance with the progress of activation process since the activation time of C10 is much longer and the weight loss of C10 is much larger than those of C3 sample

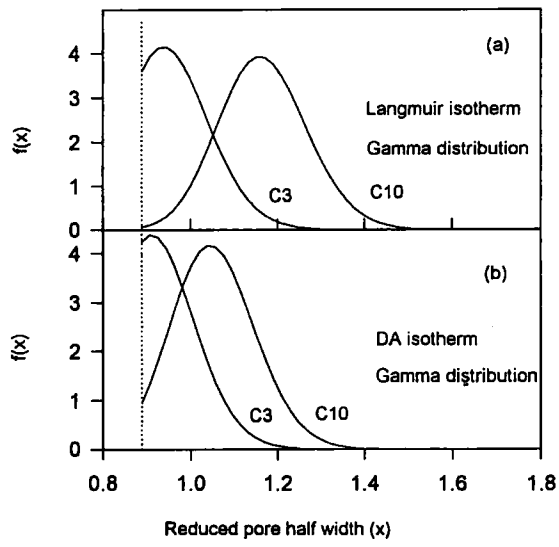

Figure 2. Micropore size distribution of two NS-ACs (a) Langmuir isotherm and Gamma distribution, (b) DA isotherm and Gamma distribution.

(Table 1). Another interesting observation from Table 1 that the micropore volumes calculated from the equilibrium data of n-butane (0.29 cc/g for C3 and 0.62 cc/g for C10) are higher than (about 1.3 times) the experimental values obtained from nitrogen adsorption at liquid nitrogen temperature. This may point to the fact the diffusion of nitrogen molecules at 77 K is so restricted that the data collected may not reflect the true equilibrium behaviour.

Figure 2(b) shows the MPSDs obtained from local DA isotherm ($n = 3$) with Gamma distribution. Compared with the MPSDs derived from local Langmuir isotherm, the MPSDs for DA local isotherm shifts to smaller pore size range.

Fitting was also carried out with the Gaussian distribution, and although it can reasonably correlate the experimental data, is not a good choice since the MPSD parameters don't seem to reflect the structure of carbon samples. The derived standard deviation δ, a measurement of heterogeneity, is less than 0.001 for both samples, a value far too small to be accepted.

The MPSD parameters in Table 2 obtained from local Langmuir isotherm and Gamma distribution are then used to derive adsorption energy distribution with Eq. (12). The full pore size range accessible to adsorbate is taken into account because for each sample the fraction of MPSD located in the pore half-width range of $(0.8885\sigma_{12}, \sigma_{12})$ is significant, especially for the C3 activated carbon sample. This is different from other studies (Jagiello and Schwarz, 1992, 1993; Hu and Do, 1994) in which the MPSDs in Section 1 are very small and was neglected in those studies. To obtain the overall adsorption energy distribution, the energy distributions from both sections at the same energy level are calculated using spline interpolation method and then summed together.

Figure 3 shows the adsorption energy distributions of n-butane on each carbon sample, in which the X-axis is the adsorption energy reduced with respect to U_s^*. It can be seen that the difference between two samples is significant. For n-butane the adsorption energy distribution on the C3 sample is concentrated in the high energy range with an average energy of 20.3 kJ/mole, while for the C10 sample the energy distribution is more dispersed with an average energy of 18.9 kJ/mole. The energy distribution curves of C3 and C10 also reflect the progress of activation on the carbon structure in which the smaller micropores with high adsorption potential is widened to the larger pores with lower adsorption potential.

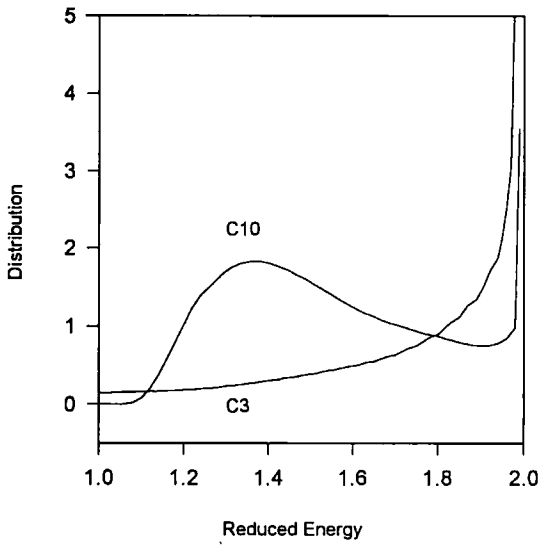

Figure 3. The reduced adsorption energy distribution of n-butane on two NS-ACs.

4.2. *MPSD and Dynamics*

Surface diffusion is an activation process which plays an important role in overall adsorption dynamics. The activation energy of surface diffusion is proportional to the adsorption energy (Yang et al., 1994). In the present work, we take this ratio as 1/2 because many systems having the van der Waals type of bonding have this value. From the adsorption energy distribution (Fig. 3) we calculate the mean activation energy of surface diffusion for the sample C3 as 10.2 kJ/mole, while it is 9.5 kJ/mole for the C10 sample. Although the mean activation energy for surface diffusion are comparable to each other, their energy distributions are quite significantly different and hence the surface flux is different.

Observing the energy distribution of these two samples in Fig. 3, we would expect that the surface diffusion of n-butane on C10 sample is faster than that on C3 sample because the C10 sample has lower energy barrier. However, the adsorption capacity of C3 sample is only about 40% of that of C10 sample, and this will compensate somewhat for its slower surface diffusion. The experimental results of adsorption dynamics of n-butane on these carbon samples are presented in Figs. 4 and 5. From these figures it can be seen that the uptake rate of n-butane on C10 is faster than that on C3. This means that the surface diffusion influences the overall adsorption kinetics more strongly than the

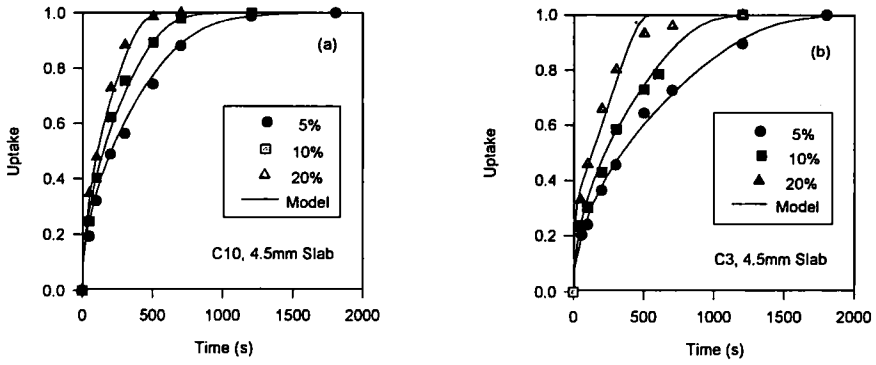

Figure 4. Adsorption dynamics of n-butane on two NS-ACs in large pellets.

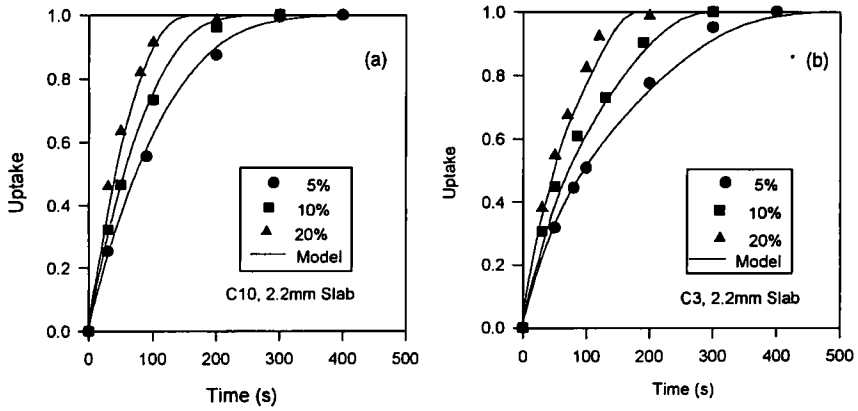

Figure 5. Adsorption dynamics of n-butane on two NS-ACs in small pellets.

adsorption capacity. The same result was observed in the studies of Ahmadpour and Do (1995).

The HMSD/HMSMD models are used to simulate the adsorption dynamics on two carbon samples. It had been shown that the micropore resistance is negligible in slab pellets with the length larger than 4 mm (Gray and Do, 1990), therefore, HMSD model is employed to simulate the n-butane adsorption dynamics on each carbon sample in large pellets (4.5 mm full length slab). The only parameter which has to be optimised in this model is the surface diffusivity at zero loading and zero energy level ($D_{\mu 0}$). The model fittings are shown in Figs. 4, which are reasonably good for n-butane uptake on each carbon sample.

For smaller pellets (2.2 mm full length slab) the micropore resistance can not be neglected. Therefore, the parameter $D_{\mu 0}$ obtained from HMSD model are used in HMSMD model to simulate the adsorption dynamics. The parameter to be derived in this model is the diffusion length in microparticle R_μ/β, a measure of the micropore resistance. The model fittings (Fig. 5) for n-butane adsorption dynamics in these small pellets are also good.

Table 4 shows the fitted parameters for n-butane adsorption dynamics on each carbon sample. Due to the difference in MPSDs, the surface diffusivity of n-butane on C10 is much larger than that of C3 (about two times), while the micropore resistance of C10 is much smaller than that of C3 (reflected in R_μ/β). This is entirely consistent with the structure of the sample C3 and C10. The sample C3 being less activated is expected to yield lower surface diffusivity and more

Table 4. Dynamics data of two nutshell activated carbons.

Sample	Size of pellets	Model used	$D_{\mu 0}$ (10^9 m^2/s)	R_μ/β (m)
C3	4.5 mm	HMSD	2.185	
	2.2 mm	HMSMD	2.185	1.120E−5
C10	4.5 mm	HMSD	4.107	
	2.2 mm	HMSMD	4.107	6.152E−6

resistance in the micropore than the sample C10 which is more activated. Do and Do (1993) had shown that equilibria information alone may not be sufficient for the complete study of MPSD and dynamics studies is needed to provide an additional tool to understand the solid structure better. The present work shows that this is the case and suggests that equilibrium and dynamics must be studied together for the better understanding of the micropore size distribution.

5. Conclusion

Activated carbons made from Macadamia nutshell by CO_2 physical activation process are of different pore structures and thus exhibit different equilibrium and dynamics properties. The micropore network is the main source of surface heterogeneity and is characterised by the distribution of slit-shaped micropores in which the adsorption potential is described by the Lennard-Jones' 10-4 potential minimum. The local Langmuir isotherm and Gamma pore size distribution are found to be a good combination, since the parameters extracted can well represent the structural differences as well as the adsorption equilibrium and dynamics behaviours on carbon samples. The combination of DA equation with Gamma pore size distribution results in the MPSDs with smaller mean pore size. The Gaussian distribution function is found to be unable to work with either isotherm equation because the parameters obtained fail to properly characterise the adsorbents. The adsorption energy distribution derived from the MPSD is more asymmetric and can be used in HMSD/HMSMD models to simulate adsorption dynamics.

Nomenclature

a	Ratio of diffusion energy to adsorption energy	0.5
b_0	Adsorption affinity at zero energy level	kpa^{-1}
C10	Activated carbon derived from nutshell with higher surface area	
C3	Activated carbon derived from nutshell with lower surface area	
C_b	Bulk phase concentration of gas phase	mole/cc
C_{im}	Imaginary gas phase concentration inside micropore	
C_μ	Adsorbed phase concentration	mole/cc
$C_{\mu 0}$	Maximum adsorbed concentration	mole/cc
C_p	Pore phase concentration	mole/cc
D_p	Pore diffusivity	m^2/s
D_μ	Surface diffusivity	m^2/s
$D_{\mu 0}$	Surface diffusivity at zero energy level	m^2/s
e	Adsorption energy	J/mole
E	Reduced adsorption energy	
$E(r)$	Adsorption energy inside the pores with radius r	J/mole
E_0	Characteristic energy in DR equation	J/mole
J_P	Pore flux	$mole/m^2/s$
J_μ	Surface flux	$mole/m^2/s$
k_m	Film mass transfer coefficient	
P	Gas phase pressure	kPa
P_s	Saturation pressure	kPa
Q	Distribution parameter $= q^*\sigma_{12}$	
q	Gamma distribution parameter	
R	Macropore radius	m
R_μ	Micropore radius	m
r	Pore half-width	m
r_β	Ratio of micropore radius to Macropore radius	
r_{min}	Minimum pore half-width accessible to adsorbate with zero adsorption potential	m
r^*	Mean radius of Gaussian distribution	m
s	Geometric factor 0, 1, 2, for slab, cylinder and sphere	
s_μ	Geometric factor for microparticle 0, 1, 2, for slab, cylinder and sphere	
T	Temperature	K
t	Time	s
$U_p(z)$	Pore potentials at distance z	J/mole
U_s^*	Potential well depth of single graphite lattice	J/mole
U_r^{min}	Potential minimum in pore with half-width r	
$V_{(T)}$	Liquid molar volume at temperature T	cc/mole
W_0	Microporosoty of activated carbon	cc/g
x	Reduced pore half width	r/σ_{12}
z	Distance between adsorbate and pore wall	m

Greek Symbols

β^2	Ratio of the zero surface diffusivity in the microparticle coordinate to that in the particle coordinate	
δ	Standard deviation	
γ	Distribution parameter	
σ_{12}	Collision diameter	m
Γ	Gamma function	
ε_M	Macroporosity	

Acknowledgment

This project is supported by the Australian Research Council.

References

Ahmadpour, A. and D.D. Do, "The Preparation of Active Carbons From Coal by Chemical and Physical Activation," *Carbon*, **34**, 471–479 (1996).

Ahmadpour, A. and D.D. Do, "Characterisation of Modified Activated Carbons: Equilibria and Dynamics Studies," *Carbon*, **33**, 1393–1398 (1995).

Chen, Y.D. and R.T. Yang, "Diffusion of Oxygen, Nitrogen and Their Mixtures in Carbon Molecular Sieve," *AIChE J.*, **40**, 577–585 (1994).

Do, D.D. and H.D. Do, "Effect of Micropore Size Distribution on the Surface Diffusivity in Microporous Solids," *Chem. Eng. Sci.*, **48**, 2625–2642 (1993).

Dubinin, M.M., *Zh. Fiz. Khimii*, **39**, 135 (1965).

Dubinin, M.M., "Fundamentals of the Theory of Adsorption in Micropores of Carbon Adsorbents: Characteristics of Their Adsorption Properties and Microporous Structures," *Carbon*, **27**, 457–467 (1989).

Everett, D.H. and J.C. Powl, "Adsorption in Slit-Like and Cylindrical Micropores in the Henry's Law Region," *J. Chem. Soc., Faraday Trans.*, **72**, 619–636 (1976).

Gray, P.G. and D.D. Do, "Adsorption Dynamics of SO_2 on a Single Large Activated Carbon Particle," *Chem. Eng. Commun.*, **96**, 141–154 (1990).

Hu, X. and D.D. Do, "Role of Energy Distribution in Multicomponent Sorption Kinetics in Bidispersed Solid," *AIChE J.*, **39**, 1628–1635 (1993).

Hu, X. and D.D. Do, "Effect of Surface Heterogeneity on the Sorption Kinetics of Gases in Activated Carbon, Pore Size Distribution vs Energy Distribution," *Langmuir*, **10**, 3296–3302 (1994).

Hu, X. and D.D. Do, "Multicomponent Adsorption Kinetics of Hydrocarbons onto Activated Carbon: Contribution of Micropore Resistance," *Chem. Eng. Sci.*, **48**, 1317–1323 (1993).

Jagiello, J. and A. Schwarz, "Energetic and Structural Heterogeneity of Activated Carbons Determined Using Dubinin Isotherms and An Adsorption Potential in Model Micropores," *J. Colloid and Interface Sci.*, **154**, 225–237 (1992).

Jagiello, J. and A. Schwarz, "Relationship Between Energetic and Structural Heterogeneity of Microporous Carbons Determined on the Basis of Adsorption Potentials in Model Micropores," *Langmuir*, **9**, 2513–2517 (1993).

Jaroniec, M. and R. Madey et al., "Comparison of Adsorption Methods for Characterising the Microporosity of Activated Carbons," *Carbon*, **27**, 77–83 (1989).

Krishna, R., "A Unified Approach to the Modelling of Intraparticle Diffusion in Adsorption Processes," *Gas Sep. & Purif.*, **7**, 91–104 (1993).

Nguyen, C., A. Ahmadpour, and D.D. Do, "Effects of Gasifying Agents on the Characterisation of Nutshell Derived Activated Carbon," *Adsorption Sci & Tech.*, **12**, 247–258 (1995).

Russell, B.P. and M.D. LeVan, "Pore Size Distribution of BPL Activated Carbon Determined by Different Methods," *Carbon*, **32**, 845–885 (1994).

Ruthven, D.M., *Principles of Adsorption and Adsorption Process*, Wiley, New York, 1984.

Stoeckli, H.F. et al., "Recent Developments in the Dubinin Equation," *Carbon*, **27**, 125–128 (1989).